Kinetic and equilibrium modelling of MTBE (Methyl tert-butyl ether) adsorption on ZSM-5 zeolite: Batch and column studies

Yunhui Zhang[a*]; *Fei Jin*[b]; *Zhengtao Shen*[c]; *Rod Lynch*[a]; *Abir Al-Tabbaa*[a]

[a]Department of Engineering, University of Cambridge, Cambridge, CB2 1PZ, United Kingdom
[b]School of Engineering, University of Glasgow Singapore, 138683, Singapore
[c]Department of Earth and Atmospheric Sciences, University of Alberta, T6G 2E3, Canada

AUTHOR INFORMATION

***Corresponding Author**

Tel: +44- (0) 7821464199

E-mail address: yz485@cam.ac.uk.

Abstract

The intensive use of methyl tert-butyl ether (MTBE) as a gasoline additive has resulted in serious environmental problems due to its high solubility, volatility and recalcitrance. The feasibility of permeable reactive barriers (PRBs) with ZSM-5 type zeolite as a reactive medium was explored for MTBE contaminated groundwater remediation. Batch adsorption studies showed that the MTBE adsorption onto ZSM-5 follows the Langmuir model and obeys the pseudo-second-order model with an adsorption capacity of 53.55 $mg \cdot g^{-1}$. The adsorption process reached equilibrium within 24 h, and MTBE was barely desorbed with initial MTBE concentration of 300 $mg \cdot L^{-1}$. The mass transfer process is found to be primarily controlled by pore diffusion for MTBE concentrations from 100 to 600 $mg \cdot L^{-1}$. pH has little effect on the maximum adsorption capacity in the pH range of 2-10, while the presence of nickel reduces the capacity with Ni concentrations of 2.5-25 $mg \cdot L^{-1}$. In fixed-bed column tests, the Dose-Response model fits the breakthrough curve well, showing a saturation time of ~320 min and a removal capacity of ~18.71 $mg \cdot g^{-1}$ under the conditions of this study. Therefore, ZSM-5 is an extremely effective adsorbent for MTBE removal and has a huge potential to be used as a reactive medium in PRBs.

Key words: MTBE, ZSM-5 zeolite, batch adsorption, mass transfer mechanism, fixed-bed column test

1. Introduction

Methyl tert-butyl ether (MTBE) was a widely used gasoline additive. Although it has been banned in some countries, the residual contamination exists due to fugitive emissions from petrol refineries and petrol filling stations, emissions from vehicles, petrol spills and leaking storage tanks [1]. The last report of UST (Underground Storage Tank) performance measures indicated that approximately 13.6% of UST releases remained to be cleaned up in the year of 2015 [2]. In addition, it is reported that tanks did not pass the leakage tests in some regions [3] and probably affected the aquifers or groundwater where the remediation has always been considered to be difficult, expensive and slow [4]. Considering that groundwater is an important source of water supply worldwide, especially for where there is a shortage of surface water or lakes, groundwater remediation is of great significance for water supply and human health worldwide.

MTBE has an unpleasant odour and harmful effects on the respiratory and nerve systems of living things although its carcinogenesis remains unclear [5]. MTBE pollution in the environment mainly exists in groundwater and aquifers rather than in surface water and soil due to its high solubility, volatility and recalcitrance and has received increasing attention worldwide [6].

MTBE is found to be resistant to chemical and biological degradations [7] and therefore immobilisation may be a more suitable treatment. In-situ technologies have attracted increased attention in terms of groundwater and aquifer remediation of MTBE ascribed to their low costs and simple operation over conventional technologies such as pump and treat. Permeable reactive barriers (PRBs) are one of the most promising in-situ treatments [8]. Barriers filled with reactive materials are constructed across the flow path of a contaminant

plume [9]. As the fluid moves through the PRBs, contaminants are degraded or trapped by reactive materials through physical, chemical and/or biological processes.

The reactive medium is the key component of PRBs and its selection is dependent on the nature of the target contaminants and hydro-geological site conditions. ZSM-5, a high-silica MFI type zeolite, has been found to be effective for MTBE adsorption due to its hydrophobicity and suitable pore size [10,11]. Although the use of natural or modified zeolites has been extensively studied [12,13] due to their good adsorptivity, stability and renewability, research on the use of ZSM-5 as the reactive material in PRBs is limited. Vignola et al. [14,15] utilised ZSM-5 for in-situ PRBs located close to a coastal refinery to remediate MTBE and hydrocarbons contaminated groundwater and the results showed that MTBE was reduced to under 10 μg/L for about 100 days. Faisal and Hmood [16] used ZSM-5 in laboratory-scale PRBs to remove cadmium from a contaminated shallow aquifer and the PRBs started to saturate after ~120 h under conditions tested. For the design of PRBs, it is crucial to figure out the detailed adsorption process of MTBE onto ZSM-5, which necessitates an understanding of kinetics, isotherms, the rate-limiting step, influencing factors and the desorption behaviour [17]. However, to date, most studies have focused on the relationship between the properties of ZSM-5 and its adsorption capacities for MTBE, and there is a lack of research on the detailed adsorption and desorption features.

This work aims to explore the detailed mass transfer mechanisms, adsorption and desorption features of ZSM-5 and to examine its feasibility in PRBs for MTBE removal. Adsorption kinetics, isotherms and desorption kinetics are presented and the diffusion parameters were modelled to assess the rate-limiting step of the entire batch adsorption process. Due to the fact that the real groundwater conditions, such as pH and the existence of heavy metals, are

complex and may have an effect on MTBE adsorption, different influencing factors, such as initial solution pH, solid/liquid ratio and the presence of nickel ions, are explored in this study. In addition, fixed-bed column experiments are performed to evaluate the effectiveness of ZSM-5 as a reactive medium in PRBs.

2. Materials and methods

2.1 Materials

MTBE and ZSM-5 were purchased from Fisher Scientific and Acros Organics, respectively. The physicochemical properties of ZSM-5 were obtained from the supplier and are given in Table 1. Figure 1 was adapted [18] and presented the molecular structure and dimensions of ZSM-5. There are two pore systems in ZSM-5, one consisting of zig-zag channels of the near-circular cross-section and another consisting of straight channels of the elliptical shape. Other chemicals used (HCl, NaOH, $NiSO_4 \cdot 6H_2O$) were obtained from Fisher Scientific with A.R. grade.

Table 1 The physicochemical properties of ZSM-5

Surface area ($m^2 \cdot g^{-1}$)	Pore size (Å)	Particle size (μm)	SiO_2/Al_2O_3	pH	CEC ($cmol \cdot kg^{-1}$)
400	5.3x5.6; 5.1x5.5	2-8	469	4.14	1.808

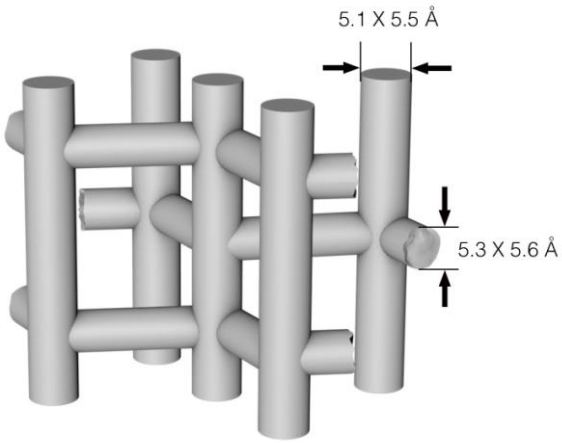

Figure 1 Molecular structure and dimensions of ZSM-5 [18]

2.2 Batch adsorption studies

2.2.1 Kinetic study

Batch kinetic studies were carried out by adding 0.1 g of ZSM-5 into 60 mL small air-tight glass bottles with minimum headspace containing 20 mL MTBE solutions with different concentrations (100, 150, 300 or 600 $mg \cdot L^{-1}$) to avoid the evaporative loss of MTBE [19]. The agitation speed was kept constant at 200 rpm in a shaker for a pre-determined time before filtration using a 0.45 μm glass fiber filter. The shaking time was set at 5 min, 10 min, 20 min, 30 min, 3 h, 6 h, 12 h, 24 h, 48 h, 72 h and 96 h.

2.2.2 Equilibrium study

To study the adsorption isotherm of MTBE onto ZSM-5, 0.1 g of ZSM-5 was added to 20 mL solutions containing different MTBE concentrations (20, 60, 100, 150, 300, 600 and 800 $mg \cdot L^{-1}$). From the kinetic study, it was found that 24 h was required to reach equilibrium. The following influencing factors were considered:

(1) The effect of solution pH was examined by varying the initial pH of the solutions from pH 2 to 10. The pH was adjusted using 0.1 M HCl or 0.1 M NaOH. The initial MTBE concentration was fixed at 300 $mg \cdot L^{-1}$ with ZSM-5 dosage of 0.1 g/20 mL.

(2) The effect of solid/liquid ratio was evaluated by adding different amounts of ZSM-5 (0.02, 0.05, 0.08, 0.1, 0.2 and 0.3 g) to 20 mL of 300 $mg \cdot L^{-1}$ MTBE solutions.

(3) The effect of the existence of nickel ions was examined by mixing 0.1 g ZSM-5 with 300 $mg \cdot L^{-1}$ MTBE solutions containing various concentrations of Ni (0, 2.5 and 25 $mg \cdot L^{-1}$) at pH = 7.

In addition, after the batch adsorption experiments for 24 h (with initial MTBE concentration of 300 $mg \cdot L^{-1}$ and ZSM-5 dosage of 0.1 g). The samples were centrifuged and the supernatant was decanted. Desorption kinetic experiments were performed by the addition of 20 mL deionized water with a stirring speed of 200 rpm for various time periods (same with those of adsorption kinetic tests).

2.3 Fixed-bed column tests

Fixed-bed column tests were conducted on a laboratory scale to simulate the application of ZSM-5 in PRBs for MTBE removal. The tests were performed using 2 cm inner diameter and 10 cm high Pyrex glass columns. Columns were packed with a mixture of ZSM-5 (5%) and model sandy soil. Model soil samples were made by mixing 92% sand with 3% clay and 5% slit represented by kaolin and silica flour, respectively. This model soil is classified as sand [20]. The water content is 10% and the density is about 2 $g \cdot cm^{-3}$. The porosities of model soil and the mixture are 32.41% and 31.63%, respectively. The total bed length is 9 cm and initial MTBE concentration is 300 $mg \cdot L^{-1}$. The flow rate is kept constant at 2 $mL \cdot min^{-1}$. Aqueous samples were collected at regular intervals and analysed for MTBE concentrations throughout the test period. From a practical point of view, the saturation time, t_s, is established when the concentration in the effluent is higher than 90% of the inlet concentration [21]. The breakthrough time here, t_b, is established when the MTBE concentration in the effluent reaches 50% of the inlet concentration.

2.4 Analytical methods

MTBE was analyzed using a gas chromatograph (Agilent 6850 Series) with a flame ionisation detector (GC-FID) by an ambient headspace technique at 20°C as used in our previous study [22]. Each headspace sample was measured in triplicate. Blank experiments were carried out under identical conditions with adsorption experiments for all the MTBE

concentrations and showed negligible influence of the MTBE volatility on the test results. The concentration of Ni^{2+} was measured by inductively coupled plasma-optical emission spectrometry (ICP-OES) (Perkin-Elmer, 7000DV) after dilution and acidification. OriginPro 8.5 software was used to perform data fitting and modelling and output fitting values, standard errors, correlation coefficient (R^2) and Akaike information criterion (AIC) values. The AIC and R^2values were used in this study to compare predictions with the experimental data and find out the best fitting model. AIC is an estimator of the relative quality of statistical models for a given set of data and provides a means for model selection. The model with higher R^2 and lower AIC values is preferred.

3. Results and discussion

3.1 Adsorption kinetics

The pseudo-first-order and pseudo-second-order models were used to describe the kinetics of MTBE adsorption onto ZSM-5. The fitting of the experimental kinetics data is presented in Figure 2 and Table 2. Where q_e and q_t are the amount of adsorbate adsorbed at equilibrium and time t ($mg \cdot g^{-1}$), respectively, k_1 and k_2 are the rate constants of pseudo-first-order adsorption (h^{-1}) and pseudo-second-order adsorption ($g \cdot mg^{-1} \cdot s^{-1}$), respectively.

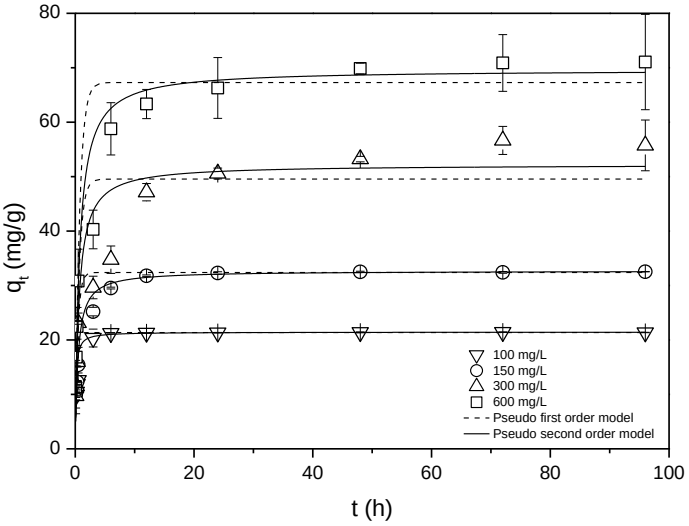

Figure 2 The fitting of pseudo-first-order and pseudo-second-order models for MTBE adsorption onto ZSM-5 at different initial concentrations

Table 2 Kinetics model parameters for MTBE adsorption onto ZSM-5 at different MTBE concentrations

Models	Equations	Parameters	Initial MTBE concentration ($mg \cdot L^{-1}$)			
			100	150	300	600
Pseudo-first-order	$q_t = q_e(1 - e^{-k_1 t}$	q_e ($mg \cdot g^{-1}$)	21.35±0.10	32.40±0.20	49.55±2.94	67.29±2.40
		k_1 (h^{-1})	5.57±0.74	2.35±0.80	1.59±0.11	1.40±0.38
		AIC	43.59	51.04	50.95	29.98
		R^2	0.94	0.84	0.95	0.92
Pseudo-second-order	$q_t = \frac{q_e^2 k_2 t}{1 + q_e k_2 t}$	q_e ($mg \cdot g^{-1}$)	21.44±0.07	32.68±0.09	52.19±1.56	69.64±1.68
	$t_{\frac{1}{2}} = \frac{1}{k_2 q_e}$	k_2 ($g \cdot mg^{-1} \cdot h^{-1}$)	0.38±0.04	0.067±0.01	0.03±0.00	0.021±0.00
		$t_{1/2}$ (s)	437.23	1644.07	2090.22	2461.75
		AIC	34.44	31.41	35.91	20.22
		R^2	0.97	0.97	0.99	0.97

It was shown in Figure 2 that the adsorption of MTBE onto ZSM-5 was found to be rapid at the initial period and then plateaued with the increasing contact time. It was found that 24 h was deemed sufficient to ensure equilibrium for all the concentrations, and the equilibrium time increased with the increase of the initial MTBE concentration. From Table 2, it was found that the pseudo-second-order model was the best at all concentrations for MTBE adsorption onto ZSM-5, indicating chemisorption [23]. The amount of adsorbed MTBE increased from 21.44 $mg \cdot g^{-1}$ to 69.64 $mg \cdot g^{-1}$ by increasing the initial MTBE concentration from 100 $mg \cdot L^{-1}$ to 600 $mg \cdot L^{-1}$.

In addition, as shown in Table 2, the half-adsorption time ($t_{1/2}$) [24] was applied to further describe the adsorption equilibrium time of MTBE onto ZSM-5. $t_{1/2}$, the time required for the ZSM-5 to uptake half of the amount adsorbed at equilibrium, is typically considered as a measure of the rate of adsorption. The increase of $t_{1/2}$ values (from 437.23 s^{-1} to 2461.75 s^{-1}) indicated the increase of adsorption rate with the increase of MTBE concentration from 100 $mg \cdot L^{-1}$ to 600 $mg \cdot L^{-1}$.

3.2 Adsorption isotherms

As shown in Figure 3, the experimental data were fitted with the widely used isotherm models for solid-liquid adsorption by nonlinear regression, i.e. Langmuir, Freundlich, modified form of BET [25], Sips, Dubinin-Radushkevich and Temkin models [26]. The isotherm equations, regression analysis and model parameters are given in Table 3. For the Langmuir model, Q_0 is the maximum adsorption capacity ($mg \cdot g^{-1}$), b is the rate of adsorption ($L \cdot mg^{-1}$); C_e is the MTBE equilibrium concentration ($mg \cdot L^{-1}$), R_L is the equilibrium parameter to describe the essential characteristics of Langmuir isotherm, C_0 is the initial MTBE concentration ($mg \cdot L^{-1}$). For the Freundlich model, K_F is the adsorption capacity of the

adsorbent ($mg \cdot g^{-1}$); 1/n ranging between 0 and 1 is a measure of adsorption intensity or surface heterogeneity, and the surface of the adsorbent is more heterogeneous if its value is closer to zero. For the BET model, K_B and K_L are the equilibrium constants of adsorption for the first and upper layers ($L \cdot mg^{-1}$), respectively, q_m is the theoretical isotherm saturation capacity ($mg \cdot g^{-1}$). For the Sips model, K_s is the equilibrium constant ($L \cdot mg^{-1}$). For the Dubinin-Radushkevich model, K_D is the mean free energy of sorption per molecule of the sorbate when it is transferred to the surface of the solid from infinity in the solution ($mol^2 \cdot kJ^{-2}$), R (8.314 $J \cdot mol^{-1} \cdot K^{-1}$) is the universal gas constant and T (K) is the solution temperature. For the Temkin model, $RT/b_T=B$ ($J \cdot mol^{-1}$), which is the Temkin constant related to the heat of sorption, A_T is the equilibrium binding constant corresponding to the maximum binding energy ($L \cdot g^{-1}$).

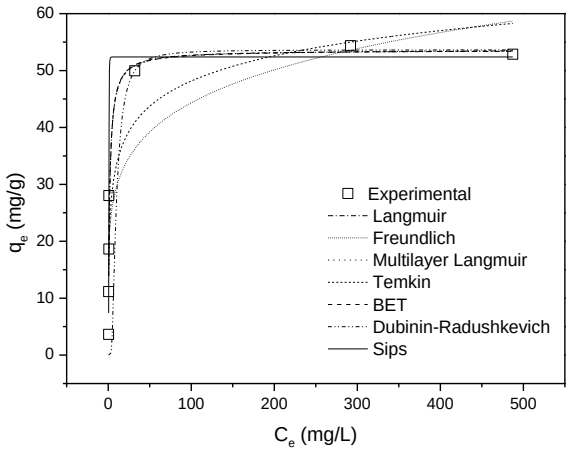

Figure 3 Isotherm plots for MTBE adsorption onto ZSM-5

Table 3 Isotherm model parameters for MTBE adsorption on ZSM-5

Models	Equations	Parameters	
Langmuir	$q_e = \frac{Q_0 b C_e}{1 + b C_e}$	Q_0 ($mg \cdot g^{-1}$)	53.55±4.07
		b ($L \cdot mg^{-1}$)	0.62±0.20
	$R_L = \frac{1}{1 + b C_0}$	R_L	0.002
		AIC	38.34

		R^2	0.90
Freundlich	$q_e = C_e^{\frac{1}{n}} K_F$	K_F (mg·g^{-1})	19.60±4.91
		1/n	0.18±0.65
		AIC	44.53
		R^2	0.76
BET	$q_e = q_m \frac{K_B C_e}{(1 - K_L C_e)(1 - K_L C_e + K_B C_$	q_m (mg·g^{-1})	53.42±8.61
		K_L (L·mg^{-1})	$8.35\times10^{-6}\pm4.66\times10^{-4}$
		K_B (L·mg^{-1})	0.62±0.27
		AIC	52.34
		R^2	0.87
Sips	$q_e = Q_0 \frac{K_S C_e^{\frac{1}{n}}}{1 + K_S C_e^{\frac{1}{n}}}$	K_S (L·mg^{-1})	2.57±1.48
		Q_0 (mg·g^{-1})	52.39±2.62
		N	0.21±0.07
		AIC	45.27
		R^2	0.95
Dubinin-Radushkevich	$q_e = q_m \exp\left(-K_D \left(RT \ln\left(1 + \frac{1}{C_e}\right)\right)^2\right.$	q_m (mg·g^{-1})	53.64±11.38
		K_D (mol^2·kJ^{-2})	$1.28\times10^{-5}\pm6.92\times10^{-5}$
		AIC	50.42
		R^2	0.43
Temkin	$q_e = \frac{RT}{b_T \ln A_T C_e}$	b_T (J·mol^{-1})	380.98±69.24
		A_T (L·g^{-1})	18.65±19.11
		AIC	41.91
		R^2	0.83

It is shown in Table 3 that the highest R^2 value indicated that the adsorption isotherm of MTBE onto ZSM-5 fits the Sips model best which is a combination of the Langmuir and Freundlich isotherms. However, the Langmuir model has the lowest AIC value. In addition, the parameters of the Sips model generally depend on the operating conditions [27]. The Sips model reduces to Freundlich isotherm at low adsorbate concentrations, and predicts a monolayer adsorption capacity characteristic of Langmuir isotherm at high concentrations which is the condition of this study. Therefore, MTBE adsorption can be described best by

the Langmuir model, indicating a monolayer and homogeneous adsorption process. The maximum adsorption capacity is 53.55 $mg \cdot g^{-1}$, and the R_L value showed that the adsorption process is favorable.

According to the results obtained, ZSM-5 could be employed as an effective adsorbent for MTBE. Table 4 gives a comparison of the adsorption capacities of MTBE on different adsorbents obtained from the literature. The adsorption kinetics of MTBE onto all these adsorbents followed the pseudo-second-order model.

Table 4 Comparison of adsorption properties of MTBE with zeolites and other adsorbents

Adsorbents	Maximum adsorption capacity ($mg \cdot g^{-1}$)	Isotherm model	Reference
nano-PFOAL$_G$	10.09	BET	[26]
nano-PFOAL$_B$	10.41	BET	[26]
diatomite	-	Freundlich	[28]
mordenite	2.94	Freundlich	[29]
carbonaceous resin (Ambersorb 572)	4.97	Freundlich	[30]
lignite	0.13	Freundlich	[31]
activated carbon	66.72	Freundlich	[31]
activated carbon	1.94	Freundlich	[29]
HDTMA-modified clinoptilolite	91.60	Langmuir	[32]
Beta, Engelhard	25.06	Langmuir	[33]
ZSM-5	0.67	Langmuir	[33]
ZSM-5	95.00	Langmuir	[34,35]
ZSM-5	53.55	Langmuir	This study

nano-PFOAL: nano-perfluorooctyl alumina

3.3 Mass transfer mechanisms

3.3.1 Transport progress in adsorption process

The mass transfer process has an impact on the adsorption equilibrium time. The mass transfer of adsorbate from the solution to the adsorption sites within the adsorbent particles is constrained by mass transfer resistances [17]. The mass transfer process generally involves four steps [36]: transport from the bulk solution to the boundary layer, film (boundary layer) diffusion, intra-particle (pore and surface) diffusion and adsorption on the interior surface of adsorbents. It is generally accepted that the first and last steps are very fast and the overall adsorption process is controlled by film diffusion and/or intra-particle diffusion [37].

3.3.2 Film diffusion

Duo to that the film diffusion influences only the beginning of the adsorption process, film mass transfer coefficients, k_f ($cm \cdot s^{-1}$), were determined from the initial part of the kinetic curve (t=0, $c=c_0$, $c_s=0$) [17] with the following equations:

$$k_f = -\frac{V_L}{a_m m_A c_0}\left(\frac{dc}{dt}\right)_{t=0}$$

$$a_m = \frac{3}{\rho_p r_p}$$

Where m_A is the adsorbent mass, V_L is the liquid volume, a_m is the total surface area related to the adsorbent mass, ρ_p is the density of adsorbent particles, r_P is the radius of adsorbent particles, and the value of r_P is 2.5×10^{-4} cm for ZSM-5 in this study, c_s is the concentration of MTBE at the external particle surface. $\left(\frac{dc}{dt}\right)_{t=0}$ can be read from the slope of the tangent in the kinetic curve by setting t=0. The calculated k_f values decreased with the increasing MTBE concentrations (2.00×10^{-5} $cm \cdot s^{-1}$ for 100 mg/L, 1.34×10^{-5} $cm \cdot s^{-1}$ for 150 mg/L, 7.20×10^{-6} $cm \cdot s^{-1}$ for 300 mg/L and 3.96×10^{-6} $cm \cdot s^{-1}$ for 600 mg/L).

3.3.3 Intra-particle diffusion

3.3.3.1 Weber and Morris intra-particle diffusion model

After the film diffusion process, the adsorbate species are transported to the solid phase through intra-particle diffusion/transport process.

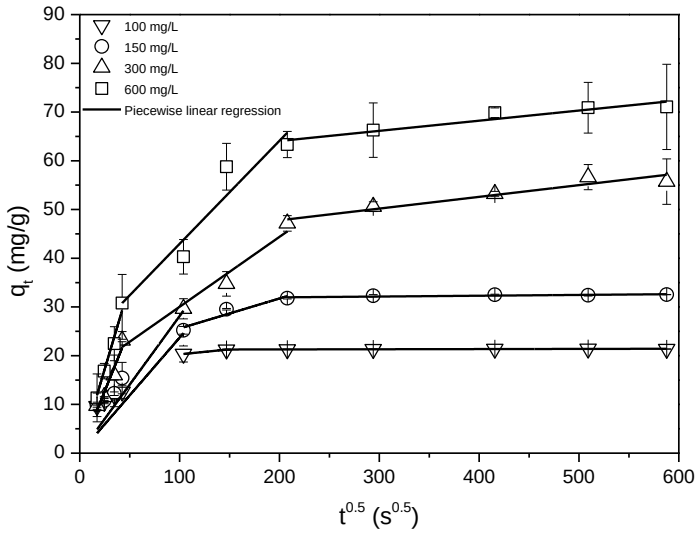

Figure 4 Intra-particle diffusion plot for MTBE adsorption onto ZSM-5 at initial MTBE concentration of 100, 150, 300 and 600 $mg \cdot L^{-1}$

Weber and Morris model was used to describe the process of intra-particle diffusion. The intra-particle diffusion rate constant, K_i ($mg \cdot g^{-1} \cdot s^{0.5}$), is defined by the following equation [38]:

$$q_t = K_i t^{0.5} + c$$

Where q_t is the amount of MTBE adsorbed ($mg \cdot g^{-1}$) at time t, and c is the intercept, giving the information about the thickness of boundary layer.

Figure 4 shows the intra-particle diffusion plot of MTBE adsorption on ZSM-5 and the piecewise linear regression results were presented in Table 5. From Figure 4, the plot of q_t against $t^{0.5}$ showed three linear portions, indicating three periods involved in the sorption

process [39,40]. The first, sharper region describes the film diffusion. In this initial stage, ZSM-5 particles are surrounded by the boundary layer and MTBE molecules have to overcome the boundary layer resistance [41]. When the external surface of ZSM-5 reached saturation, MTBE entered the inner pores of ZSM-5 and was adsorbed onto the internal adsorption sites, i.e. the second stage where intra-particle diffusion happens. The slope of the second linear portion has been defined to yield the intra-particle diffusion parameter K_2 ($mg \cdot g^{-1} \cdot s^{-0.5}$) [39]. As shown in Table 5, the values of K_i increased with the increase of MTBE concentrations, indicating that the intra-particle diffusion rate increased with higher initial MTBE concentrations. The third region is the final equilibrium stage (after 210 $s^{0.5}$) where intra-particle diffusion starts to slow down due to the extremely low adsorbate concentrations left in the solution [42].

Table 5 Piecewise linear regression parameters of intra-particle diffusion for MTBE onto ZSM-5

Parameters	Initial MTBE concentration ($mg \cdot L^{-1}$)			
	100	150	300	600
Intra-particle diffusion period	3-6 h	3-12 h	0.5-12 h	0.5-12 h
K_2 ($mg \cdot g^{-1} \cdot s^{-0.5}$)	0.02	0.06±0.02	0.14±0.02	0.21±0.04
c	18.21	19.43±2.79	15.69±2.52	21.81±5.91
R^2	1.00	0.85	0.95	0.89

It was shown in Figure 4 that all the curved plots covering the initial phase passed through the origin, suggesting that intra-particle diffusion should be the rate-controlling step in the removal of the adsorbate [40]. That is, film diffusion may be very fast and could be ignored [43]. To further judge whether the pore diffusion or surface diffusion was more important, the pore and surface diffusion coefficients were calculated as follows.

3.3.3.2 Pore diffusion

The pore diffusion coefficients largely depend on the surface properties of adsorbents. According to Bhattacharya and Venkobachar [44], the pore diffusion coefficient (D_p) can be calculated with the pseudo-first-order kinetic model. Although MTBE adsorption on ZSM-5 followed the pseudo-second-order model, the R^2 values (R^2>0.85) of pseudo-first-order model were high enough. Therefore, this method is applicable to this study to estimate pore diffusion coefficients. The equation and obtained D_p values are shown in Table 6. The values of D_p for MTBE in the present study were found to be in the order of 10^{-12}-10^{-13} $cm^2 \cdot s^{-1}$ and decreased with the increasing MTBE concentrations.

3.3.3.3 Surface diffusion

The linear driving force model (LDF model), a simplification of the surface diffusion model, was used to estimate the surface mass transfer coefficient (k_s, $cm \cdot s^{-1}$) [45]. Furthermore, the values of D_s, the surface diffusion coefficient, are also calculated to compare with those of D_P to assess the rate-limiting step of the adsorption process. The equations and obtained values of D_s and k_s are shown in Table 6. Where A_s is the total external surface area of all adsorbent particles, q_s is the adsorbed amount at external particle surface which can be calculated from the adsorption isotherm, $\bar{q}$ is the mean adsorbent loading. $c_s(t)$ at time t can be read from the kinetic curve by setting $c_s(t)=c(t)$ (fast film diffusion), and $q_s(t)$ related to $c_s(t)$ can be calculated by the isotherm equation. To find an average value for k_s, the procedure was repeated for different pairs of values (c, t).

The values of D_s for MTBE in the present study were found to be in the order of 10^{-13} $cm^2 \cdot s^{-1}$ and increased with the increase of MTBE concentration from Table 6. This may be due to that the increasing MTBE concentration increased the surface loading, thereby leading to an

increase of adsorbate mobility and a decrease of the adsorption energy [17]. This fell well within the magnitudes for chemisorption system (10^{-5} to 10^{-13} $cm^2 \cdot s^{-1}$) [46]. Since surface diffusion and pore diffusion act in parallel and competitively, the faster process dominates and determines the total adsorption rate. As a result, pore diffusion was the rate-limiting step for MTBE adsorption on ZSM-5.

In addition, Bangham's equation was used for MTBE adsorption to test the role of diffusion [47].

$$loglog\left(\frac{C_0}{C_0 - C_s q_t}\right) = log\left(\frac{K_b C_s}{2.303V}\right) + \alpha log t$$

Where C_0 is the initial MTBE concentration ($mg \cdot L^{-1}$), C_s is the solid/liquid ratio ($g \cdot L^{-1}$), q_t is the amount of MTBE at time t ($mg \cdot g^{-1}$), α and K_b are constants. $loglog\left(\frac{C_0}{C_0 - C_s q_t}\right)$ was plotted against log t in Figure 5. The fitted linearity indicated the applicability of Bangham's model (R^2>0.91), and showed that the diffusion of MTBE into the pores of ZSM-5 mainly controlled the adsorption process.

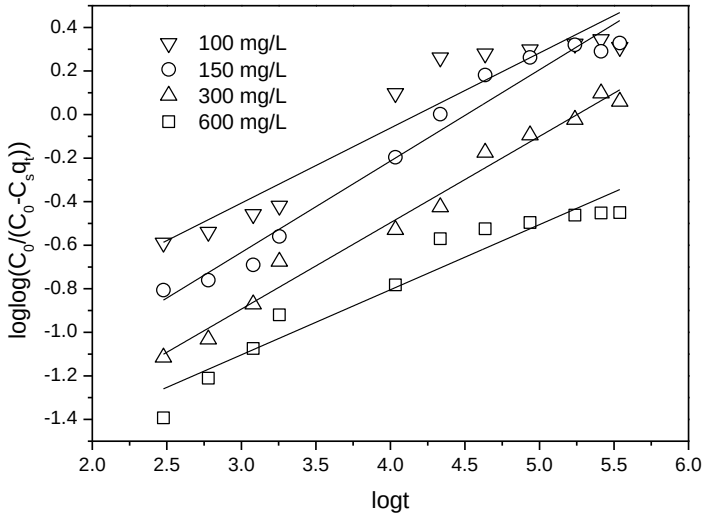

Figure 5 Bangham plot for MTBE adsorption on ZSM-5 at different initial concentrations

Table 6 Mass transfer and diffusion coefficients for MTBE adsorption on ZSN-5 at different initial concentrations

		Initial MTBE concentration ($mg \cdot L^{-1}$)			
		100	150	300	600
D_p ($cm^2 \cdot s^{-1}$)	$t_{\frac{1}{2}} = \frac{0.03{r_p}^2}{D_p}$	42.88×10^{-13}	11.41×10^{-13}	8.97×10^{-13}	7.62×10^{-13}
k_s (s^{-1})	$k_s = -\frac{k_f}{\rho_p}\frac{[c(t)-c_s(t)]}{[q_s(t)-\bar{q}(t)]}$ $c_s(t) = c(t) + \frac{V_L}{m_A k_f a_m}(\frac{\partial c}{\partial t})_t$ $A_s = a_m m_A = \frac{3m_A}{\rho_p r_p}$	5.15×10^{-9}	6.27×10^{-9}	12.97×10^{-9}	15.16×10^{-9}
D_s ($cm^2 \cdot s^{-1}$)	$D_s = \frac{k_s r_p}{5}$	2.57×10^{-13}	3.13×10^{-13}	6.49×10^{-13}	7.58×10^{-13}

3.4 Effect of initial solution pH

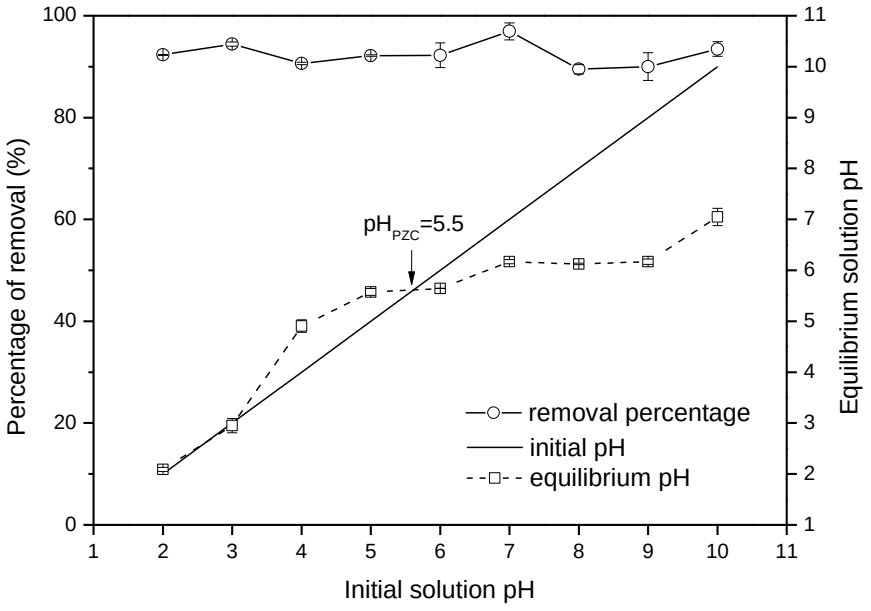

Figure 6 The effect of initial solution pH on the percentage of MTBE removal (the equilibrium solution pH is also presented)

Solution pH controls the electrostatic interactions between the adsorbent and adsorbate. Therefore, it determines the adsorbent surface charge and the dissociation or protonation of organic weak electrolytes [48]. As shown in Figure 6, the pH at PZC (point of zero charge) of ZSM-5 was around 5.5. This means that when pH values were above 5.5, the surface of ZSM-5 was negatively charged, which was favourable for cation exchange. It was also shown that the removal percentage of MTBE onto ZSM-5 remained at ~90 % and was barely affected by the change of initial solution pH. The same phenomenon was reported for the adsorption of other organics [49,50]. This may be due to that ZSM-5 in this study has little potential for the ion exchange considering its high SiO_2/Al_2O_3 ratio and low CEC (Cation Exchange Capacity) value as shown in Table 1. In addition, MTBE is a weakly polar molecule, and the protonation of the functional groups is not high enough to compete with the sorption of water molecules due to the still strong H-bonding abilities of these groups compared with their deprotonated counterparts [49], which leads to the weak electrostatic interaction between ZSM-5 and MTBE.

3.5 Effect of solid to liquid ratio

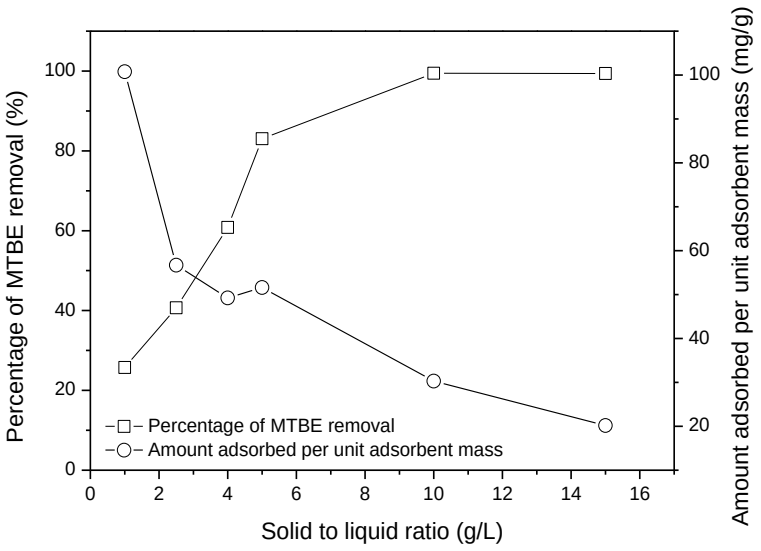

Figure 7 The effect of solid/liquid ratio on MTBE adsorption onto ZSM-5

As shown in Figure 7, the percentage of MTBE removal increased significantly from 25.73% to 99.42% with the increase of ZSM-5 dosage from 1 $g \cdot L^{-1}$ to 10 $g \cdot L^{-1}$ and remained constant beyond 10 $g \cdot L^{-1}$. The amount of MTBE adsorbed per unit adsorbent mass at equilibrium decreased across the ZSM-5 dosage range of 1-15 $g \cdot L^{-1}$.

3.6 Effect of the existence of Ni (II)

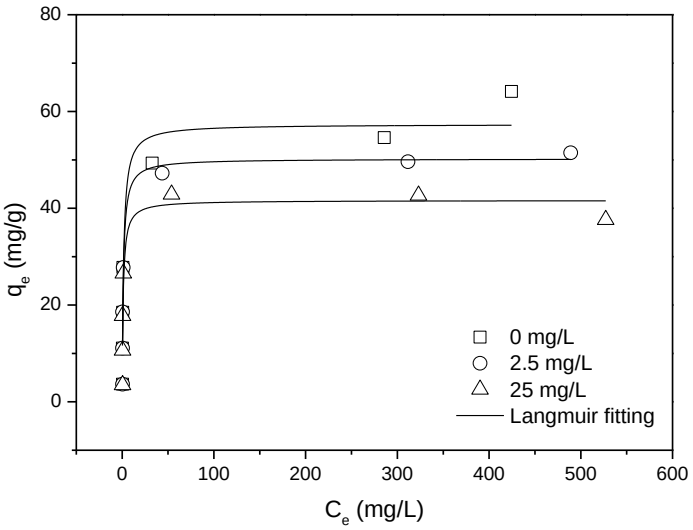

Figure 8 MTBE adsorption isotherms onto ZSM-5 with different concentrations of Ni (II) (0, 2.5 and 25 $mg \cdot L^{-1}$) (pH=7)

Effect of Ni(II) on the sorption of MTBE on ZSM-5 was evaluated in the presence of different concentrations of Ni^{2+}. As shown in Figure 8, according to Langmuir model, the maximum adsorption capacities decreased with the increasing Ni^{2+} concentrations (57.36 $mg \cdot g^{-1}$ for 0 $mg \cdot L^{-1}$ Ni^{2+}, 50.22 $mg \cdot g^{-1}$ for 2.5 $mg \cdot L^{-1}$ Ni^{2+} and 41.63 $mg \cdot g^{-1}$ for 25 $mg \cdot L^{-1}$ Ni^{2+}, respectively). This indicated that the existence of Ni (II) had a suppression effect on MTBE adsorption onto ZSM-5. This may be attributed to both direct competition for sorption sites and pore blockage mechanism [49]. The surface complexation of hydrated Ni^{2+} may

perturb surface chemistry and/or pore structure of ZSM-5. Similarly, the surface complexation of Cu^{2+} was also reported to have a suppression effect on the sorption of organics to wood charcoal [49]. In addition, considering the ionic radii of Ni^{2+} (0.7 Å), hydrated Ni^{2+} and thermochemical radii of SO_4^{2-} (2.58 Å), the addition of cations and anions and their hydrated products may lead to the increasing ionic strength and the occupation of the pores of ZSM-5. However, the detailed competitive adsorption mechanism between Ni^{2+} (and other heavy metal contaminants) and MTBE is complex and warrants further studies.

3.7 Desorption kinetics

The desorption characteristics are an important factor to evaluate the effectiveness of an adsorbent. The results showed that MTBE was hardly desorbed (<2%) after 96 h with initial MTBE concentration of 300 $mg \cdot L^{-1}$. This means that the adsorption between ZSM-5 and MTBE is very strong and ZSM-5 is an effective and suitable adsorbent for MTBE.

3.8 Fixed-bed column tests

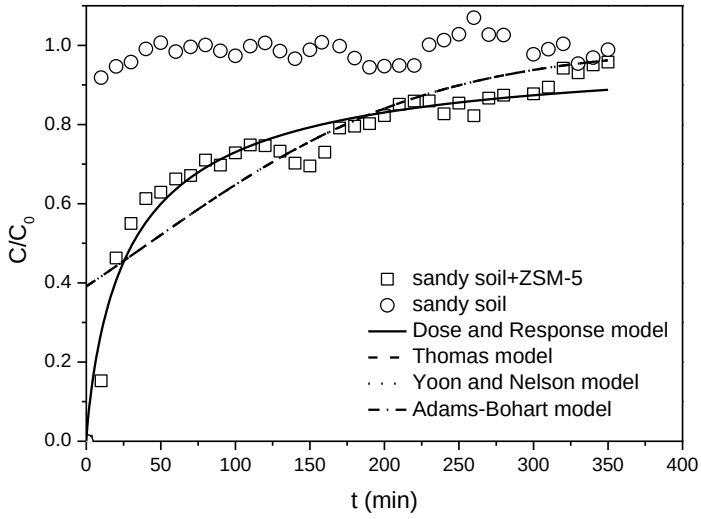

Figure 9 The experimental and predicted breakthrough curves for the adsorption of MTBE on sand and sand-ZSM-5 mixture at an inlet MTBE concentration of 300 $mg \cdot L^{-1}$

As the adsorption and desorption performance of ZSM-5 in batch adsorption studies was good for MTBE removal, ZSM-5 was used as a reactive medium in fixed-bed column tests to simulate its application in PRBs. Column tests were carried out with a total operational time of 350 min to reach saturation in this study.

From the breakthrough curves in Figure 9, the saturation time was about 320 min while the control sample was saturated at the very beginning (within 10 minutes). This indicated that sandy soil had almost no adsorption ability for MTBE and the addition of 5% ZSM-5 can improve the removal performance significantly. The breakthrough time (C/C_0=0.5) was about 25 min in this study.

Adams-Bohart model, Thomas model, Yoon-Nelson model and Dose-Response model were applied to predict the breakthrough curves and determine column kinetic parameters. The equations and calculated parameters are listed in Table 7. Where v is the linear flow rate ($cm \cdot min^{-1}$), V is the volume of the effluent (L), Q is the flow rate which circulates through the column ($mL \cdot min^{-1}$), N_0 is the saturation concentration ($mg \cdot L^{-1}$), C and C_i are the solute concentration and inlet metal concentration in the liquid phase ($mg \cdot L^{-1}$), respectively, Z is the bed depth in the column (cm), k_{AB} and K_{Th} are the constants, m is the mass of sorbent (g), τ is the time required for 50% adsorbate breakthrough (min), q_0 is the maximum concentration of the solute in the solid phase ($mg \cdot g^{-1}$), a is the constant of the Dose-Response model, b is the concentration at which half of the maximum response occurs, and Y is the response. Among these models, Dose-Response model showed the best agreement with the experimental data (R^2=0.95). From the integral Dose-Response fitting curve, the total quantity of MTBE removal is 52.37 mg, although 210 mg MTBE in total passed through the column. Therefore,

the removal capacity was ~18.71 mg·g^{-1} and ~25% MTBE was removed under the conditions of this study.

Table 7 Mathematic model parameters for the adsorption of MTBE onto ZSM-5 in fixed-bed column tests

Models	Equations	Parameters	
Adams-Bohart	$\frac{C}{C_i} = \frac{e^{k_{AB}C_i t}}{e^{(k_{AB}N_0 Z/v)} - 1 + e^{k_{AB}C_i t}}$	k_{AB} (L·mg^{-1}·min^{-1})	3.51×10^{-5}±4.67×10^{-6}
		N_0 (mg·L^{-1})	1902.84±150.59
		R^2	0.74
Thomas	$\frac{C}{C_i} = \frac{1}{1 + e^{\frac{k_{Th}}{Q}(q_0 m - C_i V)}}$	k_{Th} (mL·mg^{-1}·min^{-1})	0.035±0.005
		q_0 (mg·g^{-1})	9.00±2.54
		R^2	0.74
		q_{total} (mg)	25.2
Yoon and Nelson	$\frac{C}{C_i} = \frac{1}{1 + e^{k_{YN}(\tau - t)}}$	k_{YN} (min^{-1})	0.011±0.001
		τ_{cal} (min)	42.01±11.83
		τ_{exp} (min)	25
		R^2	0.74
Dose-Response	$Y = \frac{C}{C_i} = 1 - \frac{1}{1 + (\frac{C_i V}{q_0 m})^a}$	a	0.86±0.05
		b	0.062
		q_0 (mg·g^{-1})	6.69±0.56
	$b = V_{(50\%)} = \frac{q_0 m}{C_i}$	R^2	0.95

4. Conclusions

The detailed mass transfer mechanisms, adsorption and desorption features of ZSM-5 for MTBE removal were systematically discussed in this study. The conclusions are as follows.

(1) Kinetics and isotherm studies indicate that ZSM-5 can be effectively employed for MTBE adsorption in both batch and column tests.

(2) The adsorption follows the Langmuir model and obeys the pseudo-second-order model, suggesting a monolayer and homogeneous chemisorption process. 24 h is required to

reach adsorption equilibrium. MTBE is barely desorbed with the initial MTBE concentration of 300 mg·L^{-1}.

(3) In terms of the mass transfer mechanisms, pore diffusion is the main rate-limiting step for the entire adsorption process, and film diffusion is very fast for MTBE concentrations from 100 to 600 mg/L.

(4) The initial solution pH has little effect on the adsorption process in the pH range of 2-10, while the existence of nickel ions suppresses the adsorption of MTBE with Ni concentrations of 2.5-25 mg·L^{-1}.

(5) In the fixed-bed column tests, the breakthrough curve could be described by Dose-Response model and the saturation time is 320 min under the conditions of this study. The removal capacity is ~18.71 mg·g^{-1} with a flow rate of 2 mL·min^{-1}. Therefore, ZSM-5 is a potential and effective reactive medium for MTBE removal in PRBs and further study will be conducted to assess the effect of different operational conditions in column tests.

Acknowledgements

The authors are grateful to China Scholarship Council (CSC) for the financial help of the PhD studentship for the first author and to the Killam Trusts for providing the Izaak Walton Killam Memorial Postdoctoral Fellowship to the third author.

References

[1] WHO, Methyl tertiary-Butyl Ether (MTBE) in drinkingwater, Background document for development of WHO guidelines for drinking-water quality, 2005.

[2] US-EPA, O.o.U.S.T, Semiannual report of UST performance measures-End of fiscal year 2015 (October 1, 2014-September 30, 2015), Environmental Protection Agency, 2015.

[3] P.S. Maravanki, E.G. Picco, G.I. Servetti, Riesgo de Contaminación Ambiental en SASH (Sistema de Almacenamiento Subterráneo de Hidrocarburos) asociado a la calidad de los controles en Argentina, in: 2◦ Simposio Argentino sobre Riesgo Ambiental, UTN, Córdoba, Argentina, 2011.

[4] R.C. Pepino Minetti, H.R. Macaño, J. Britch, M.C. Allende, In situ chemical oxidation of BTEX and MTBE by ferrate: pH dependence and stability, J. Hazard. Mater. 324 (2017), 448-456.

[5] E.R. Mancini, A. Steen, G.A. Rausina, D.C.L. Wong, W.R. Arnold, F.E. Gostomski, T. Davies, J.R. Hockett, W.A. Stubblefield, K.R. Drottar, T.A. Springer, P. Errico, MTBE ambient water quality criteria development: A public/private partnership, Environ. Sci. Technol. 36 (2) (2002) 125-129.

[6] B.D. Lindsey, J.D. Ayotte, B.C. Jurgens, L.A. Desimone, Using groundwater age distributions to understand changes in methyl tert-butyl ether (MtBE) concentrations in ambient groundwater, Northeastern United States, Sci. Total Environ. 579 (2017) 579-587.

[7] S. Mohebali, Degradation of methyl t-butyl ether (MTBE) by photochemical process in nanocrystalline TiO_2 slurry: mechanism, by-products and carbonate ion effect, J. Environ. Chem. Eng. 1(4) (2013) 1070-1078.

[8] US EPA, Performance Assessment of a Permeable Reactive Barrier for Ground Water - Remediation Fifteen Years after Installation, Publication No. EPA/600/F-13/324, 2013.

[9] O. Gibert, T. Rötting, J.L. Cortina, J. de Pablo, C. Ayora, J. Carrera, J. Bolzicco, In-situ remediation of acid mine drainage using a permeable reactive barrier in Aznalcollar (Sw Spain), J. Haz. Mats. 191(1) (2011) 287-295.

[10] M.A. Anderson, Removal of MTBE and other organic contaminants from water by sorption to high silica zeolites, Environ. Sci. Technol. 34(4) (2000) 725-727.

[11] I. Levchuk, A. Bhatnagar, M. Sillanpää, Overview of technologies for removal of methyl tert-butyl ether (MTBE) from water, Sci. Total Environ. 476 (2014) 415-433.

[12] T.M. Statham, S.C. Stark, I. Snape, G.W. Stevens, K.A. Mumford, A permeable reactive barrier (PRB) media sequence for the remediation of heavy metal and hydrocarbon contaminated water: A field assessment at Casey Station, Antarctica, Chemosphere. 147 (2016) 368-375.

[13] G. Neupane, R.J. Donahoe, Attenuation of trace elements in coal fly ash leachates by surfactant-modified zeolite, J. Haz. Mats. 229 (2012) 201-208.

[14] R. Vignola, U. Cova, F. Fabiani, G. Grillo, M. Molinari, R. Sbardellati, R. Sisto, Remediation of hydrocarbon contaminants in groundwater using specific zeolites in full-scale pump&treat and demonstrative permeable barrier tests, Stud. Surf. Sci. Catal. 174 (2008) 573-576.

[15] R. Vignola, R. Bagatin, D. Alessandra De Folly, C. Flego, M. Nalli, D. Ghisletti, R. Sisto, Zeolites in a permeable reactive barrier (PRB): One year of field experience in a refinery groundwater—Part 1: The performances, Chem. Eng. J. 178 (2011) 204-209.

[16] A.A. Faisal, Z.A. Hmood, Groundwater protection from cadmium contamination by zeolite permeable reactive barrier, Desalin Water Treat. 53(5) (2015) 1377-1386.

[17] E. Worch, Adsorption technology in water treatment: fundamentals, processes, and modeling, Walter de Gruyter, 2012.

[18] A. Dyer, An introduction to zeolite molecular sieves, Australia: John Wiley & Sons, 1988.

[19] S. Hong, H. Zhang, C.M. Duttweiler, A.T. Lemley, Degradation of methyl tertiary-butyl ether (MTBE) by anodic Fenton treatment, J. Hazard. Mater. 144 (2007), 29-40.

[20] B.J. Cosby, G.M. Hornberger, R.B. Clapp, T. Ginn, A statistical exploration of the relationships of soil moisture characteristics to the physical properties of soils, Water Resour. Res. 20(6) (1984) 682-690.

[21] M. Calero, F. Hernáinz, G. Blázquez, G. Tenorio, M.A. Martín-Lara, Study of Cr (III) biosorption in a fixed-bed column, J. Haz. Mats. 171(1) (2009) 886-893.

[22] M.S.M. Chan, R.J. Lynch, Photocatalytic degradation of aqueous methyl-tert-butyl-ether (MTBE) in a supported-catalyst reactor, Environ. Chem. Lett. 1 (2003), 157-160.

[23] Z. Shen, F. Jin, F. Wang, O. McMillan, A. Al-Tabbaa, Sorption of lead by Salisbury biochar produced from British broadleaf hardwood, Bioresour. Technol. 193 (2015) 553-556.

[24] W.J. Weber, J.C. Morris, Kinetics of adsorption on carbon from solution, J. Sanit. Eng. Div. 89(2) (1963) 31-60.

[25] A. Ebadi, J.S.S. Mohammadzadeh, A. Khudiev, What is the correct form of BET isotherm for modeling liquid phase adsorption? Adsorption. 15(1) (2009) 65-73.

[26] A. Mirzaei, A. Ebadi, P. Khajavi, Kinetic and equilibrium modeling of single and binary adsorption of methyl tert-butyl ether (MTBE) and tert-butyl alcohol (TBA) onto nano-perfluorooctyl alumina, Chem. Eng. J. 231 (2013) 550-560.

[27] A.B. Pérez-Marín, V.M. Zapata, J.F. Ortuno, M. Aguilar, J. Sáez, M. Lloréns, Removal of cadmium from aqueous solutions by adsorption onto orange waste, J. Haz. Mats. 139(1) (2007) 122-131.

[28] M. Aivalioti, I. Vamvasakis, E. Gidarakos, BTEX and MTBE adsorption onto raw and thermally modified diatomite, J. Haz. Mats. 178(1) (2010) 136-143.

[29] H.W. Hung, T.F. Lin, C. Baus, F. Sacher, H.J. Brauch, Competitive and hindering effects of natural organic matter on the adsorption of MTBE onto activated carbons and zeolites, Environ. Technol. 26(12) (2005) 1371-1382.

[30] H.W. Hung, T.F. Lin, Adsorption of MTBE from contaminated water by carbonaceous resins and mordenite zeolite, J. Haz. Mats. 135(1) (2006) 210-217.

[31] M. Aivalioti, D. Pothoulaki, P. Papoulias, E. Gidarakos, Removal of BTEX, MTBE and TAME from aqueous solutions by adsorption onto raw and thermally treated lignite, J. Haz. Mats. 207 (2012) 136-146.

[32] S.K. Ghadiri, R. Nabizadeh, A.H. Mahvi, S. Nasseri, H. Kazemian, A.R. Mesdaghinia, S. Nazmara, Methyl tert-butyl ether adsorption on surfactant modified natural zeolites, Iranian J. Environ. Health. Sci. Eng. 7(3) (2010) 241-252.

[33] L. Abu-Lail, J.A. Bergendahl, R.W. Thompson, Adsorption of methyl tertiary butyl ether on granular zeolites: Batch and column studies, J. Hazard. Mater. 178 (2010), 363-369.

[34] A. Martucci, I. Braschi, C. Bisio, E. Sarti, E. Rodeghero, R. Bagatin, L. Pasti, Influence of water on the retention of methyl tertiary-butyl ether by high silica ZSM-5 and Y zeolites: A multidisciplinary study on the adsorption from liquid and gas phase, RSC Adv. 5 (2015), 86997-87006.

[35] E. Rodeghero, L. Pasti, E. Sarti, G. Cruciani, R. Bagatin, A. Martucci, Temperature-induced desorption of methyl tert-butyl ether confined on ZSM-5: An in situ synchrotron XRD powder diffraction study, Minerals 7 (2017), 34.

[36] W.J. Weber, Evolution of a technology, J. Sanit. Eng. Div. 110(5) (1984) 899-917.

[37] S. Mahdavi, N. Amini, The role of bare and modified nano nickel oxide as efficient adsorbents for the removal of Cd^{2+}, Cu^{2+}, and Ni^{2+} from aqueous solution, Environ. Earth Sci. 75(23) (2016) 1468-1482.

[38] T. Furusawa, J.M. Smith, Intra-particle mass transport in slurries by dynamic adsorption studies, AIChE J. 20(1) (1974) 88-93.

[39] M.H. Kalavathy, T. Karthikeyan, S. Rajgopal, L.R. Miranda, Kinetic and isotherm studies of Cu (II) adsorption onto H_3PO_4-activated rubber wood sawdust, J. Colloid Interface Sci. 292(2) (2005) 354-362.

[40] B.H. Hameed, M.I. El-Khaiary, Batch removal of malachite green from aqueous solutions by adsorption on oil palm trunk fibre: Equilibrium isotherms and kinetic studies, J. Haz. Mats. 154(1) (2008) 237-244.

[41] G. McKay, M.S. Otterburn, J.A. Aga, Fuller's earth and fired clay as adsorbents for dyestuffs, Water Air Soil Pollut. 24(3) (1985) 307-322.

[42] F.C. Wu, R.L. Tseng, R.S. Juang, Comparisons of porous and adsorption properties of carbons activated by steam and KOH, J. Colloid Interface Sci. 283(1) (2005) 49-56.

[43] E. Tütem, R. Apak, C.F. Ünal, Adsorptive removal of chlorophenols from water by bituminous shale, Water Res. 32(8) (1998) 2315-2324.

[44] A.K. Bhattacharya, C. Venkobachar, Removal of cadmium (II) by low cost adsorbents, J. Environ. Eng. 110(1) (1984) 110-122.

[45] E. Glueckauf, Theory of chromatography, Part 10: Formulae for diffusion into spheres and their application to chromatography, T. Faraday. Soc. 51 (1955) 1540-1551.

[46] B. Al Duri, G. Mckay, Basic dye adsorption on carbon using a solid-phase diffusion model, Chem. Eng. J. 38(1) (1988) 23-31.

[47] C. Aharoni, M. Ungarish, Kinetics of activated chemisorption. Part 2. Theoretical models. J. Chem. Soc., Perkin Trans. 1, 73 (1977) 456-464.

[48] C. Moreno-Castilla, Adsorption of organic molecules from aqueous solutions on carbon materials, Carbon. 42(1) (2004) 83-94.

[49] J. Chen, D. Zhu, C. Sun, Effect of heavy metals on the sorption of hydrophobic organic compounds to wood charcoal, Environ. Sci. Technol. 41(7) (2007) 2536-2541.

[50] D. Zhu, S. Hyun, J.J. Pignatello, L.S. Lee, Evidence for π-π electron donor-acceptor interactions between π-donor aromatic compounds and π-acceptor sites in soil organic matter through pH effects on sorption, Environ. Sci. Technol. 38(16) (2004) 4361-4368.

Table

Table 1 The physicochemical properties of ZSM-5

Surface area ($m^2 \cdot g^{-1}$)	Pore size (Å)	Particle size (μm)	SiO_2/Al_2O_3	pH	CEC ($cmol \cdot kg^{-1}$)
400	5.3x5.6; 5.1x5.5	2-8	469	4.14	1.808

Table 2 Kinetics model parameters for MTBE adsorption onto ZSM-5 at different MTBE concentrations

Models	Equations	Parameters	Initial MTBE concentration ($mg \cdot L^{-1}$)			
			100	150	300	600
Pseudo-first-order	$q_t = q_e(1 - e^{-k_1 t})$	q_e ($mg \cdot g^{-1}$)	21.35±0.10	32.40±0.20	49.55±2.94	67.29±2.40
		k_1 (h^{-1})	5.57±0.74	2.35±0.80	1.59±0.11	1.40±0.38
		AIC	43.59	51.04	50.95	29.98
		R^2	0.94	0.84	0.95	0.92
Pseudo-second-order	$q_t = \frac{q_e^2 k_2 t}{1 + q_e k_2 t}$ $t_{\frac{1}{2}} = \frac{1}{k_2 q_e}$	q_e ($mg \cdot g^{-1}$)	21.44±0.07	32.68±0.09	52.19±1.56	69.64±1.68
		k_2 ($g \cdot mg^{-1} \cdot h^{-1}$)	0.38±0.04	0.067±0.01	0.03±0.00	0.021±0.00
		$t_{1/2}$ (s)	437.23	1644.07	2090.22	2461.75
		AIC	34.44	31.41	35.91	20.22
		R^2	0.97	0.97	0.99	0.97

Table 3 Isotherm model parameters for MTBE adsorption on ZSM-5

Models	Equations	Parameters	
Langmuir	$q_e = \frac{Q_0 b C_e}{1 + bC_e}$ $R_L = \frac{1}{1 + bC_0}$	Q_0 (mg·g^{-1})	53.55±4.07
		b (L·mg^{-1})	0.62±0.20
		R_L	0.002
		AIC	38.34
		R^2	0.90
Freundlich	$q_e = C_e^{\frac{1}{n}} K_F$	K_F (mg·g^{-1})	19.60±4.91
		1/n	0.18±0.65
		AIC	44.53
		R^2	0.76
BET	$q_e = q_m \frac{K_B C_e}{(1 - K_L C_e)(1 - K_L C_e + K_B C_e)}$	q_m (mg·g^{-1})	53.42±8.61
		K_L (L·mg^{-1})	8.35×10^{-6}±4.66×10^{-4}
		K_B (L·mg^{-1})	0.62±0.27
		AIC	52.34
		R^2	0.87
Sips	$q_e = Q_0 \frac{K_S C_e^{\frac{1}{n}}}{1 + K_S C_e^{\frac{1}{n}}}$	K_S (L·mg^{-1})	2.57±1.48
		Q_0 (mg·g^{-1})	52.39±2.62
		N	0.21±0.07
		AIC	45.27
		R^2	0.95
Dubinin-Radushkevich	$q_e = q_m \exp\left(-K_D\left(RT\ln\left(1 + \frac{1}{C_e}\right)\right)^2\right)$	q_m (mg·g^{-1})	53.64±11.38
		K_D (mol^2·kJ^{-2})	1.28×10^{-5}±6.92×10^{-5}
		AIC	50.42
		R^2	0.43
Temkin	$q_e = \frac{RT}{b_T \ln A_T C_e}$	b_T (J·mol^{-1})	380.98±69.24
		A_T (L·g^{-1})	18.65±19.11
		AIC	41.91
		R^2	0.83

Table 4 Comparison of adsorption properties of MTBE with zeolites and other adsorbents

Adsorbents	Maximum adsorption capacity ($mg \cdot g^{-1}$)	Isotherm model	Reference
nano-PFOAL$_G$	10.09	BET	[26]
nano-PFOAL$_B$	10.41	BET	[26]
diatomite	-	Freundlich	[28]
mordenite	2.94	Freundlich	[29]
carbonaceous resin (Ambersorb 572)	4.97	Freundlich	[30]
lignite	0.13	Freundlich	[31]
activated carbon	66.72	Freundlich	[31]
activated carbon	1.94	Freundlich	[29]
HDTMA-modified clinoptilolite	91.60	Langmuir	[32]
Beta, Engelhard	25.06	Langmuir	[33]
ZSM-5	0.67	Langmuir	[33]
ZSM-5	95.00	Langmuir	[34,35]
ZSM-5	53.55	Langmuir	This study

nano-PFOAL: nano-perfluorooctyl alumina

Table 5 Piecewise linear regression parameters of intra-particle diffusion for MTBE onto ZSM-5

Parameters	Initial MTBE concentration ($mg \cdot L^{-1}$)			
	100	150	300	600
Intra-particle diffusion period	3-6 h	3-12 h	0.5-12 h	0.5-12 h
K_2 ($mg \cdot g^{-1} \cdot s^{-0.5}$)	0.02	0.06±0.02	0.14±0.02	0.21±0.04
c	18.21	19.43±2.79	15.69±2.52	21.81±5.91
R^2	1.00	0.85	0.95	0.89

Table 6 Mass transfer and diffusion coefficients for MTBE adsorption on ZSM-5 at different initial concentrations

		Initial MTBE concentration ($mg \cdot L^{-1}$)			
		100	150	300	600
D_p ($cm^2 \cdot s^{-1}$)	$t_{\frac{1}{2}} = \frac{0.03{r_P}^2}{D_p}$	42.88×10^{-13}	11.41×10^{-13}	8.97×10^{-13}	7.62×10^{-13}
k_s (s^{-1})	$k_s = -\frac{k_f}{\rho_P}\frac{[c(t)-c_s(t)]}{[q_s(t)-\bar{q}(t)]}$ $c_s(t) = c(t) + \frac{V_L}{m_A k_f a_m}(\frac{\partial c}{\partial t})_t$ $A_s = a_m m_A = \frac{3m_A}{\rho_P r_P}$	5.15×10^{-9}	6.27×10^{-9}	12.97×10^{-9}	15.16×10^{-9}
D_s ($cm^2 \cdot s^{-1}$)	$D_s = \frac{k_s r_P}{5}$	2.57×10^{-13}	3.13×10^{-13}	6.49×10^{-13}	7.58×10^{-13}

Table 7 Mathematic model parameters for the adsorption of MTBE onto ZSM-5 in fixed-bed column tests

Models	Equations	Parameters	
Adams-Bohart	$\frac{C}{C_i} = \frac{e^{k_{AB}C_i t}}{e^{(k_{AB}N_0 Z/v)} - 1 + e^{k_{AB}C_i t}}$	k_{AB} ($L \cdot mg^{-1} \cdot min^{-1}$)	$3.51\times10^{-5}\pm4.67\times10^{-6}$
		N_0 ($mg \cdot L^{-1}$)	1902.84±150.59
		R^2	0.74
Thomas	$\frac{C}{C_i} = \frac{1}{1 + e^{\frac{k_{Th}}{Q}(q_0 m - C_i V)}}$	k_{Th} ($mL \cdot mg^{-1} \cdot min^{-1}$)	0.035±0.005
		q_0 ($mg \cdot g^{-1}$)	9.00±2.54
		R^2	0.74
		q_{total} (mg)	25.2
Yoon and Nelson	$\frac{C}{C_i} = \frac{1}{1 + e^{k_{YN}(\tau - t)}}$	k_{YN} (min^{-1})	0.011±0.001
		τ_{cal} (min)	42.01±11.83
		τ_{exp} (min)	25
		R^2	0.74
Dose-Response	$Y = \frac{C}{C_i} = 1 - \frac{1}{1 + (\frac{C_i V}{q_0 m})^a}$	a	0.86±0.05
		b	0.062
		q_0 ($mg \cdot g^{-1}$)	6.69±0.56
	$b = V_{(50\%)} = \frac{q_0 m}{C_i}$	R^2	0.95

Figure
Click here to download Figure: Figures.docx

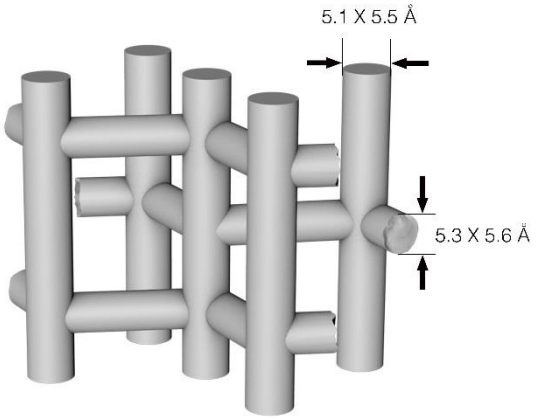

Figure 1 Molecular structure and dimensions of ZSM-5 [18]

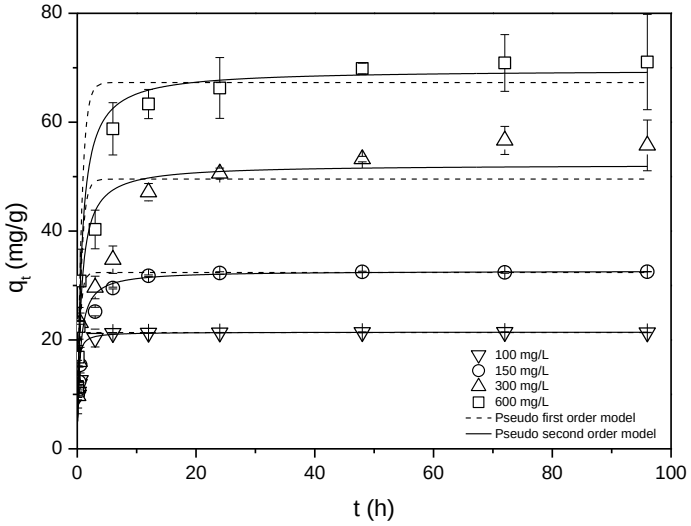

Figure 2 The fitting of pseudo-first-order and pseudo-second-order models for MTBE adsorption onto ZSM-5 at different initial concentrations

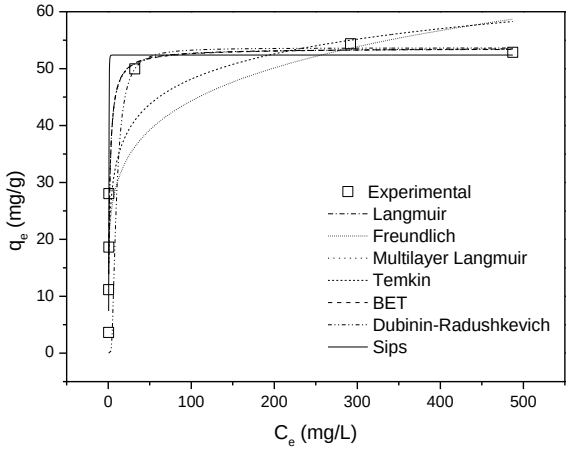

Figure 3 Isotherm plots for MTBE adsorption onto ZSM-5

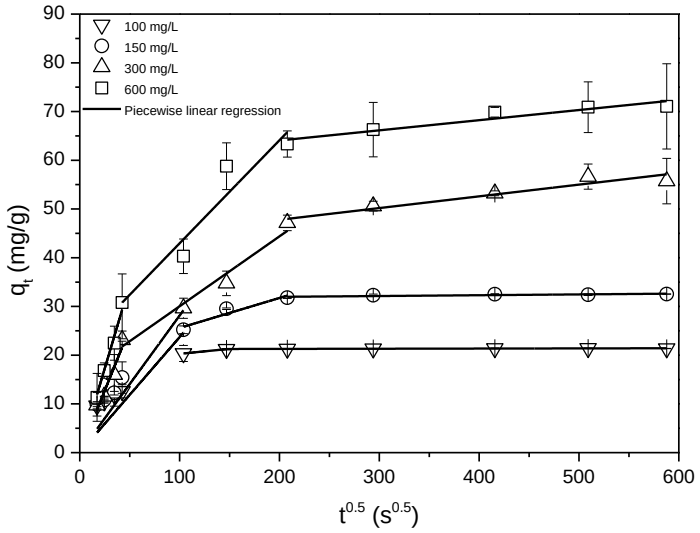

Figure 4 Intra-particle diffusion plot for MTBE adsorption onto ZSM-5 at initial MTBE concentration of 100, 150, 300 and 600 mg·L^{-1}

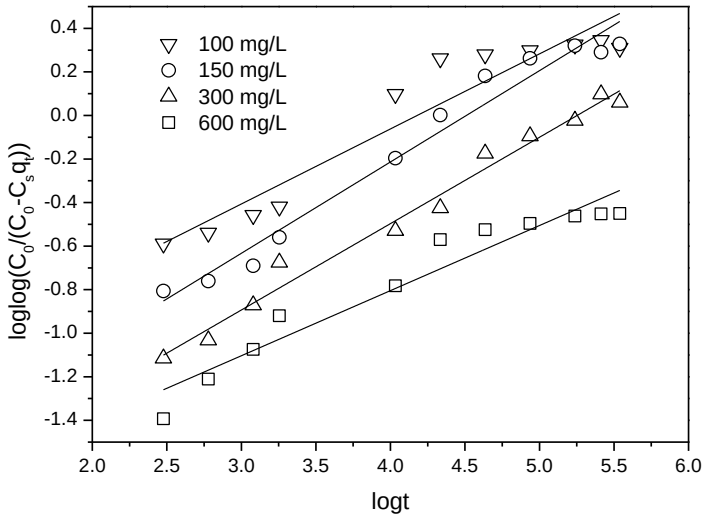

Figure 5 Bangham plot for MTBE adsorption on ZSM-5 at different initial concentrations

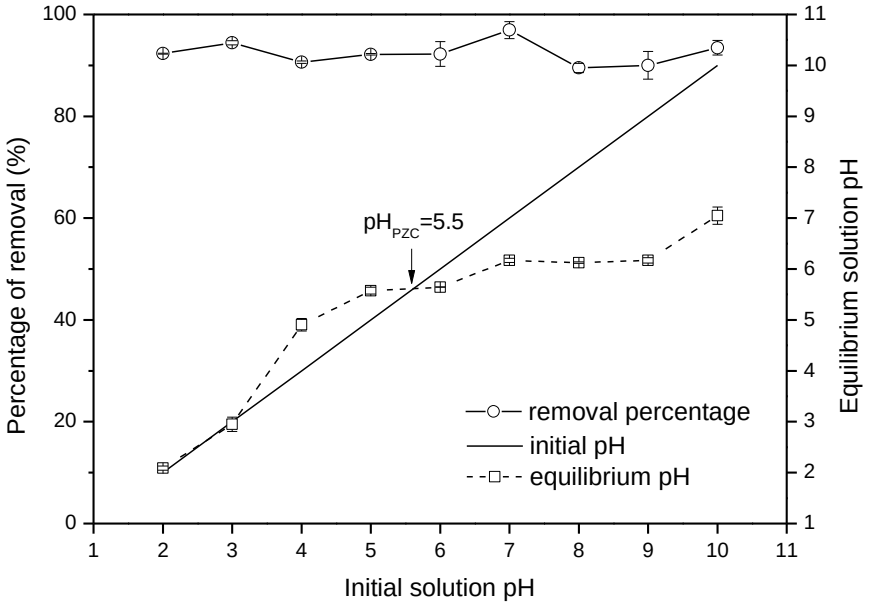

Figure 6 The effect of initial solution pH on the percentage of MTBE removal (the equilibrium solution pH is also presented)

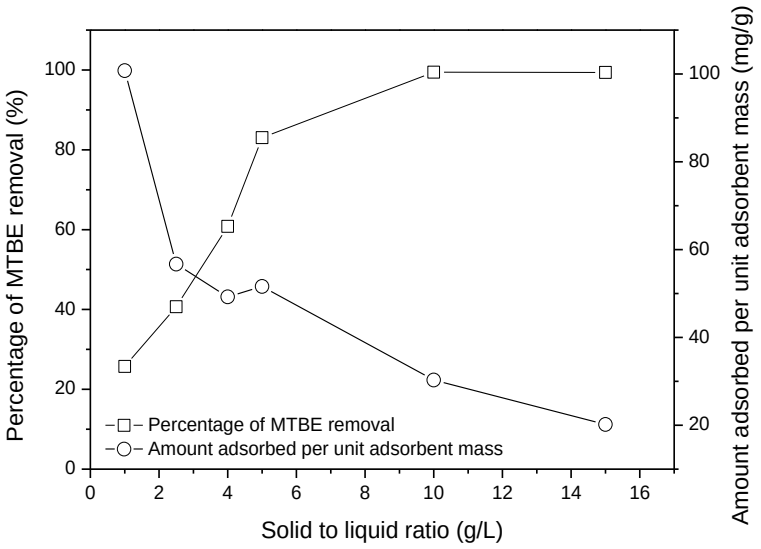

Figure 7 The effect of solid/liquid ratio on MTBE adsorption onto ZSM-5

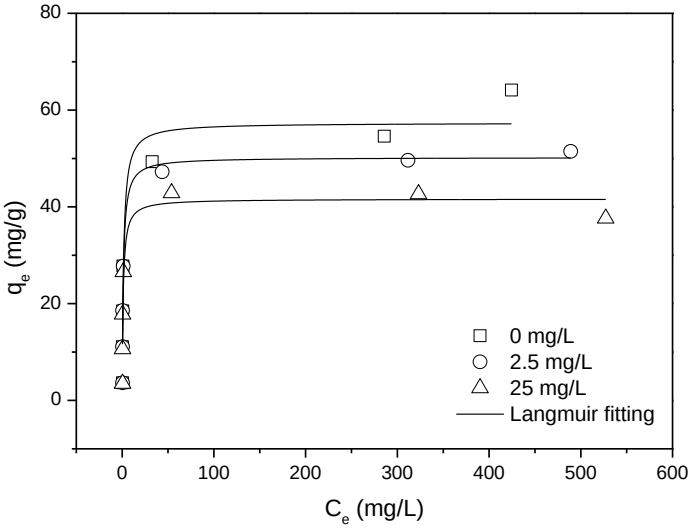

Figure 8 MTBE adsorption isotherms onto ZSM-5 with different concentrations of Ni (II) (0, 2.5 and 25 mg·L^{-1}) (pH=7)

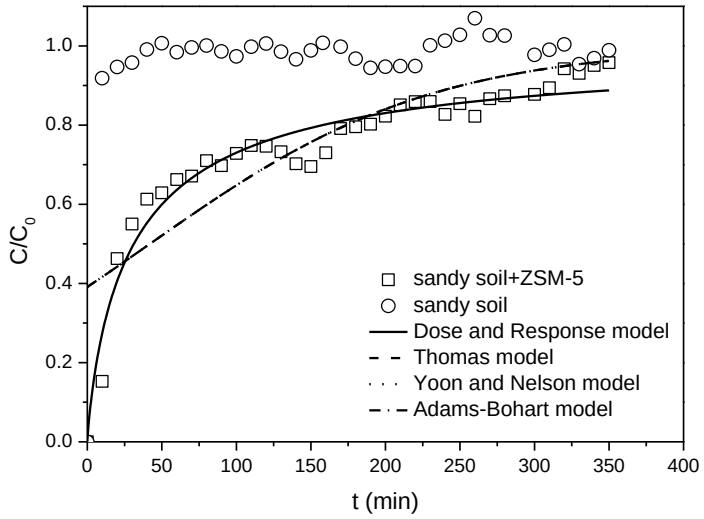

Figure 9 The experimental and predicted breakthrough curves for the adsorption of MTBE on sand and sand-ZSM-5 mixture at an inlet MTBE concentration of 300 $mg \cdot L^{-1}$

Highlights

1. The adsorption process of MTBE on ZSM-5 was explored with batch and column tests.
2. The adsorption follows the Langmuir model and obeys a pseudo-second-order model.
3. Pore diffusion is the main rate-limiting step for the entire adsorption process.
4. pH has little effect, while nickel ions suppress the adsorption process.
5. The removal capacity is ~18.71 $mg \cdot g^{-1}$ in fixed-bed column tests.

*Novelty Statement (maximum limit:100 words)

Novelty Statement

ZSM-5 has significant potential as the reactive medium in PRBs for MTBE polluted groundwater remediation due to high and strong adsorption capacity. However, there is a lack of research into detailed mass transfer mechanisms and adsorption process, which is crucial for designing adsorption systems. This study explores the mass transfer and adsorption process in detail considering the effect of pH, co-existence of heavy metals, solid/liquid ratio and MTBE concentration. Additionally, the breakthrough curve of fixed-bed column tests was obtained and modelled. The results would offer considerable insights into the applicability of ZSM-5 in PRBs for environmental remediation.